ELSEVIER

Journal of Organometallic Chemistry 515 (1996) 1–9

Journal of Organometallic Chemistry

Carbonylation of iron(II) halide in the presence of chelate diphosphine ligands. Molecular structure of a novel intermolecular adduct $[FeCl_2(dppe)_2][Fe_2(CO)_2Cl_4]$

Zheng-Zhi Zhang [a,*], Jing-Kun Zhang [b], Wei-Dong Zhang [b], Hua-Ping Xi [a], Hui Cheng [a], Hong-Gen Wang [b]

[a] *Elemento-Organic Chemistry Laboratory, Nankai University, Tianjin 300071, People's Republic of China*
[b] *Central Laboratory, Nankai University, Tianjin 300071, People's Republic of China*

Received 27 April 1995; in revised form 8 November 1995

Abstract

Treatment of tetrahydrofuran solution of $FeCl_2 \cdot 4H_2O$ or FeX_2 (X = Br, I) and chelate diphosphines L_2 [$L_2 = {}^tBuN(PPh_2)_2$, ${}^iPrN(PPh_2)_2$, $Ph_2PCH_2CH_2PPh_2$ (dppe)] with carbon monoxide at room temperature and atmospheric pressure gives *trans*-$Fe(CO)_2X_2L_2$ (X = Cl, Br, I) in high yields. Their IR, ^{31}PNMR spectra and X-ray crystallography prove that they have the structures of *trans*-carbonyls and *cis*-halogens. Reaction of $FeCl_2 \cdot 4H_2O$ and dppe with carbon monoxide gives a novel cage intermolecular adduct in which the active species of $Fe_2(CO)_2Cl_4$ is stabilized by the cage structure of $FeCl_2(dppe)_2$ in crystalline state. The structures of $Fe(CO)_2I_2[{}^tBuN(PPh_2)_2]$ (**1**) and $[FeCl_2(dppe)_2][Fe_2(CO)_2Cl_4]$ (**8**) are determined by X-ray crystallography. Compound **1** crystallizes in the space group $P\bar{1}$, with $a = 9.605(2)$, $b = 10.295(2)$, $c = 17.219(4)$ Å, $\alpha = 97.86$, $\beta = 94.98(2)$, $\gamma = 109.16(2)°$, and $Z = 2$, $R = 0.071$, $Rw = 0.080$. Compound **8** crystallizes in the space group $P\bar{1}$, with $a = 9.874(2)$, $b = 10.576(1)$, $c = 13.347(4)$ Å, $\alpha = 86.09(2)$, $\beta = 85.05(2)$, $\gamma = 81.43(1)°$, and $Z = 1$, $R = 0.078$, $Rw = 0.082$.

Keywords: Carbonylation; Adducts; Iron halides

1. Introduction

The importance of iron(0) carbonyl complexes as catalysts or promoters of organic syntheses is well known, but little attention has been paid to the study of iron(II) halides with carbonyl and phosphine ligands. Usually, these compounds can be obtained by three routes.

(a) Direct halogenation of phosphine–iron(0) carbonyls.

(b) Reaction of iron(II) carbonyl halides with phosphines.

(c) Carbonylation of iron(II)–phosphine complexes.

Route (a) is hardly controlled and the products are complicated [1–3]. Although route (b) is widely used, only *cis*-carbonyl products can be obtained [3,4]. Route (c) was initially investigated by Booth and Chatt [5]. They found that $FeCl_2(PR_3)_2$ (R_3 = $PhEt_2$, Ph_2Et, Et_3) reacted with carbon monoxide to form *cis*-carbonyl complexes $Fe(CO)_2Cl_2(PR_3)_2$, but high pressure (around 50 atm), long reaction time (3–6 days) and low yield limited its application.

Soon Manuel [6] found $FeCl_2$ could react with carbon monoxide in the presence of diphosphine ligand (dppe) to give the *cis*- or *trans*-carbonyl complex $FeCl_2(CO)_2$(dppe) in high yield at room temperature and atmospheric pressure depending on the solvent used. Recently, using an approach analogous to Manuel's, Jacobsen and Shaw [7] gave an iron(II) monocarbonyl complex containing the diphosphine ligand and dppm (dppm = $Ph_2PCH_2PPh_2$) in high yield. These studies have shown that the carbonylation of iron(II) halide in the presence of chelate diphosphines may be accomplished in high yield at room temperature and atmospheric pressure. We investigated the carbonylation of FeX_2 in the presence of certain phosphine and obtained some unprecedented results.

* Corresponding author.

SSDI 0022-328X(95)06061-8

2. Results and discussion

2.1. $RN(PPh_2)_2$ derivatives

Carbon monoxide was bubbled into THF solution of $RN(PPh_2)_2$ (R = ^{i}Pr, ^{i}Bu) and $FeCl_2 \cdot 4H_2O$ or FeX_2 (X = Br, I) at room temperature and atmospheric pressure, and $Fe(CO)_2X_2[RN(PPh_2)_2]$(**1–5**) were formed in high yield as dark green or yellow–green, air-stable, crystalline solids (Eqs. (1) and (2)).

$$Fe + X_2 \xrightarrow{THF} FeX_2 \xrightarrow[CO,THF,r.t.]{RN(PPh_2)_2} \textit{trans}\text{-}Fe(CO)_2X_2[RN(PPh_2)_2] \quad (1)$$

X = I, Br; R = ^{i}Pr, ^{i}Bu

$$FeCl_2 \cdot 4H_2O \xrightarrow[CO,THF,r.t.]{^iBuN(PPh_2)_2} \textit{trans}\text{-}Fe(CO)_2Cl_2[^iBuN(PPh_2)_2] \quad (2)$$

When the diphosphine ligand was identical, the reactivity of FeX_2 and the stability of products followed an order of I > Br > Cl, while with the same FeX_2, ^{i}BuN$(PPh_2)_2$ reacted more easily than ^{i}PrN$(PPh_2)_2$ because of the steric effect.

Reactions of different ratios of FeI_2/$RN(PPh_2)_2$ (1 : 2 or 1 : 1) resulted in the same dark green products; this is quite different from the analogous reaction of dppm in which a monocarbonyl compound was obtained [7].

The ^{31}P NMR spectra of complexes **1–5** consisted of single resonances ranging from 93.55 to 115.77 ppm, and the IR spectra showed a single carbonyl stretching band appearing in the region of 1960–2000 cm^{-1}. These results suggest that the two carbonyls lie in the *trans*-position (Fig. 1), as has been proved by X-ray crystallographic study of **1**.

2.2. Dppe derivatives

Three dppe derivatives (**6–8**) were prepared by analogous methods, summarized in Eqs. (3) and (4). The carbonylation reactivity of FeX_2 followed an order of Cl > Br > I.

$$Fe + X_2 \xrightarrow[X=I,Br]{THF} FeX_2 \xrightarrow[CO,THF,r.t.]{dppe} \textit{trans}\text{-}Fe(CO)_2X_2(dppe) \quad (3)$$

$$FeCl_2 \cdot 4H_2O \xrightarrow[CO,THF,r.t.]{dppe} \textit{trans}\text{-}[FeCl_2(dppe)_2][Fe_2(CO)_2Cl_4] \quad (4)$$

The iodide derivative (**6**) was a dark red, air-stable, crystalline solid, but the bromide derivative (**7**) was a red, little air-sensitive solid. The IR and ^{31}P NMR spectra indicated that **6** and **7** had a similar structure to complexes **1–5**.

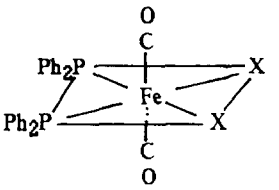

Fig. 1. The structure of complex **1**.

From $FeCl_2 \cdot 4H_2O$, yellow needle crystals of **8** were obtained, showing single absorption at 1938 cm^{-1} (assigned to γ (C≡O)) and ^{31}P NMR single resonance at 55.46 ppm. The X-ray crystallographic study of **8** indicated that it had a novel structure, as shown in Fig. 2.

Complex **A** in **8** is an adduct of Fe(II) containing two dppe. Many adducts containing two diphosphines are already known [8–11]. The complex formulated as $FeCl_2(dppe)_2$ has already been reported, but not fully characterized [12,13]. Recently, Leigh and coworkers [11] reported that $FeCl_2(dppe)_2$ did not exist, using Mössbasuer spectroscopy. However, our X-ray crystallographic study proved the existence of $FeCl_2(dppe)_2$.

Complex **B** has a novel structure. It could be regarded as two molecules of $FeCl_2$ bridged by two carbonyls. This kind of μ-CO bridging structure is rare, found in some early–late heterobimetallic (ELHB) complexes in which there are linear structures of M–C–O or M–O–C [14], but both Fe–C–O (132.9°) and Fe–O–C (119.5°) are non-linear in complex **B**.

Complex **B** in **8** could also be regarded as a dimer of $FeCl_2(CO)$. Usually, unstable carbonyl complexes $MCl_2(CO)$ display a high carbonyl absorption frequency (2150–2200 cm^{-1}) due to the donation of σ-electrons from carbonyl to the metal atom in the formation of an M–C bond. As for other $MX_2(CO)$ complexes, the interaction between Fe and CO may be best thought of as an entirely weak σ-bonded system, γ(C≡O) of **8** should appear at a high frequency. However, the bonding of the oxygen atom of carbonyl to an iron atom leads to a carbonyl stretching frequency lower than those in other $MX_2(CO)$ complexes [15–17].

Although $MCl_2(CO)$ are unstable, the complex **8** showed a significant stability in air, even when exposed for a week. The cage structure formed in the crystalline state may be responsible for this stabilization of the

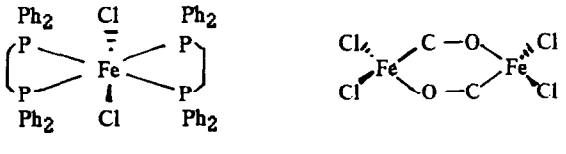

Fig. 2. The structure of complex **8**.

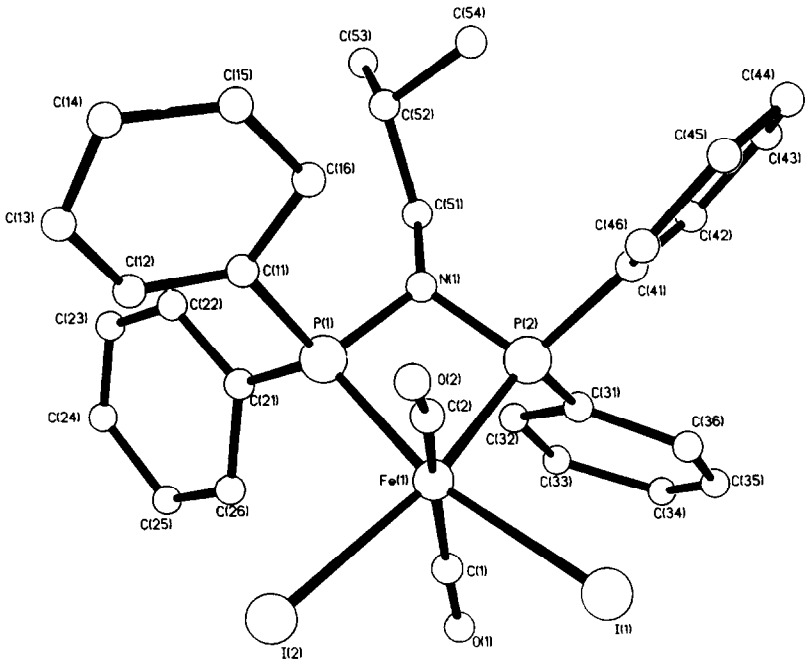

Fig. 3. Molecular structure of $Fe(CO)_2I_2$ [$^tBuN(PPh_2)_2$] (1).

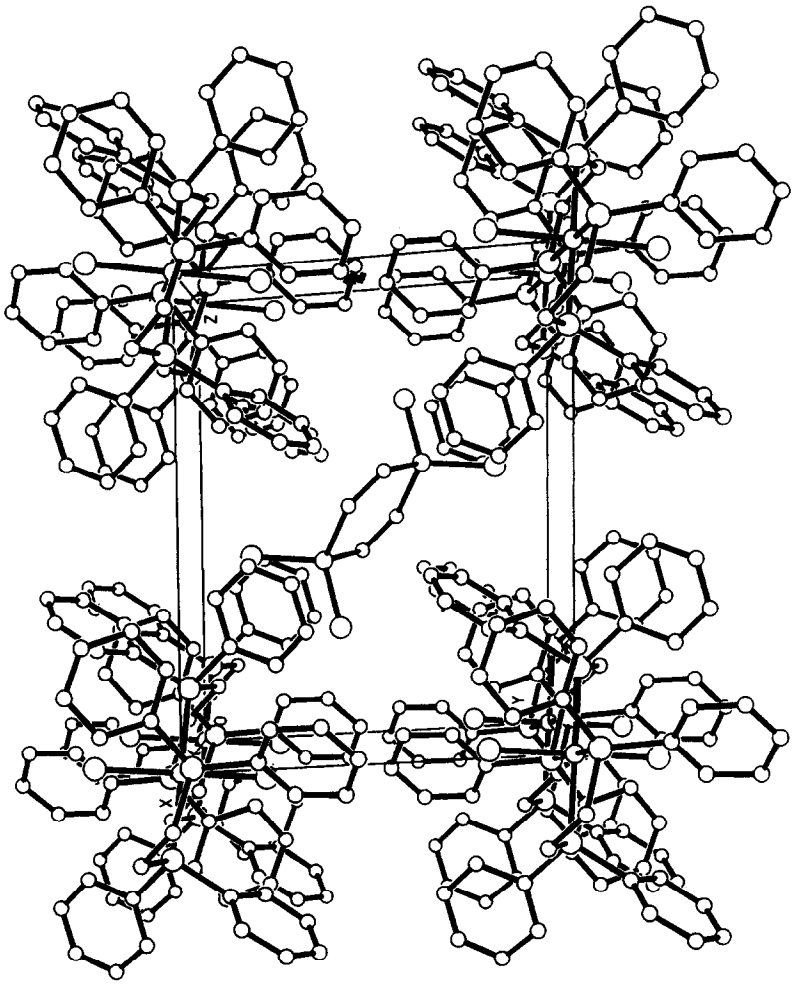

Fig. 4. Crystalline cell of $[FeCl_2(dppe)_2][Fe_2Cl_4(CO)_2]$ (8).

Table 1
Fractional coordinates and thermal parameters for non-hydrogen atoms in $Fe(CO)_2I_2[^iBuN(PPh_2)_2]$ (1)

Atom	x	y	z	B_{eq} (Å^2)
I(1)	0.3289(3)	0.0978(2)	0.7252(1)	4.44(5)
I(2)	0.0428(2)	−0.2011(2)	0.8121(1)	3.75(5)
Fe(1)	0.3059(4)	−0.1470(3)	0.7636(2)	2.50(7)
P(1)	0.3207(7)	−0.3541(6)	0.7746(4)	3.4(1)
P(2)	0.5320(7)	−0.1423(6)	0.7437(4)	3.6(1)
C(11)	0.202(3)	−0.500(3)	0.701(2)	9.5(7)
C(12)	0.070(3)	−0.592(3)	0.718(2)	11.3(9)
C(13)	−0.032(4)	−0.698(4)	0.658(2)	14(1)
C(14)	0.005(4)	−0.722(4)	0.579(2)	13(1)
C(15)	0.141(4)	−0.616(3)	0.560(2)	13(1)
C(16)	0.249(4)	−0.502(3)	0.620(2)	13(1)
C(21)	0.318(3)	−0.425(3)	0.861(2)	10.0(7)
C(22)	0.317(3)	−0.568(3)	0.859(2)	11.8(9)
C(23)	0.311(4)	−0.629(3)	0.929(2)	11.4(9)
C(24)	0.297(4)	−0.560(4)	1.002(2)	14(1)
C(25)	0.299(6)	−0.410(4)	1.008(2)	15(2)
C(26)	0.299(4)	−0.346(3)	0.938(2)	12(1)
C(31)	0.682(2)	−0.039(3)	0.822(1)	9.0(7)
C(32)	0.697(3)	−0.093(3)	0.890(2)	11.5(8)
C(33)	0.817(3)	0.003(3)	0.956(2)	11.1(8)
C(34)	0.910(4)	0.154(4)	0.945(2)	14(1)
C(35)	0.871(4)	0.190(3)	0.875(2)	14(1)
C(36)	0.762(3)	0.112(3)	0.811(2)	12(1)
C(41)	0.618(3)	−0.116(3)	0.653(1)	10.5(8)
C(42)	0.777(3)	−0.089(3)	0.658(2)	11.5(8)
C(43)	0.840(4)	−0.084(3)	0.586(2)	12(1)
C(44)	0.745(3)	−0.100(3)	0.512(2)	12.3(9)
C(45)	0.592(3)	−0.123(3)	0.515(2)	11.1(9)
C(46)	0.514(3)	−0.130(3)	0.582(1)	10.7(8)
C(1)	0.378(3)	−0.053(3)	0.862(2)	10.3(8)
C(2)	0.213(3)	−0.208(3)	0.668(2)	13.0(8)
O(1)	0.423(2)	0.016(2)	0.925(1)	9.0(6)
O(2)	0.126(3)	−0.249(2)	0.604(1)	11.9(8)
N(1)	0.498(2)	−0.313(2)	0.753(1)	7.6(5)
C(51)	0.609(3)	−0.382(3)	0.766(2)	10.9(7)
C(52)	0.587(3)	−0.509(2)	0.701(2)	12.4(9)
C(53)	0.692(3)	−0.581(3)	0.742(3)	16(1)
C(54)	0.630(5)	−0.464(4)	0.620(2)	16(1)

Anisotropically refined atoms are given in the form of the isotropic equivalent displacement parameter defined as: $\gamma\ (4/3)*[a^2 * B(1,1) + b2 * B(2,2) + c2 * B(3,3) + ab(\cos\gamma) * B(1,2) + ac(\cos\beta) * B(1,3) + bc(\cos\alpha) * B(2,3)]$.

Table 2
Selected bond lengths (Å) and angles (deg) for $Fe(CO)_2I_2[^iBuN(PPh_2)_2]$ (1)

Bond lengths			
I(1)–Fe(1)	2.637(1)	P(2)–N(1)	1.709(7)
I(2)–Fe(1)	2.638(1)	P(1)–N(1)	1.705(7)
Fe(1)–C(1)	1.79(2)	Fe(1)–P(1)	2.215(2)
Fe(1)–C(2)	1.73(1)	Fe(1)–P(2)	2.214(2)
C(1)–O(1)	1.18(1)	C(2)–O(2)	1.26(1)
Bond angles			
Fe(1)–C(1)–O(1)	175.7	P(1)–Fe(1)–C(1)	101.2
Fe(1)–C(2)–O(2)	170(1)	P(2)–Fe(1)–C(1)	90.0(3)
C(1)–Fe(1)–C(2)	165.4(5)	P(2)–Fe(1)–C(2)	100.4(4)
I(1)–Fe(1)–C(1)	85.9(3)	I(1)–Fe(1)–C(2)	82.6(3)
I(2)–Fe(1)–C(1)	85.1(3)	I(2)–Fe(1)–C(2)	87.4(4)
I(1)–Fe(1)–I(2)	97.30(4)	P(1)–Fe(1)–P(2)	71.86(9)
I(1)–Fe(1)–P(1)	166.65(8)	I(2)–Fe(1)–P(2)	164.43(9)

complex **B**. Fig. 4 shows the arrangement of **A** and **B** in a crystalline cell. Around **B**, eight **A** molecules are located to form the cage structure. However, in solution, **B** is rapidly decomposed. For example, after the CH_2Cl_2 solution of **8** was stirred for 3 h in air, the carbonyl absorption band disappeared. While, in analogous conditions, the CH_2Cl_2 solution of **6** stirred for 12 h showed no change in the carbonyl absorption intensity.

2.3. Molecular structure of 1

Fig. 3 gives the ORTEP projection of the molecule **1**, fractional coordinates of non-hydrogen atoms are given in Table 1, and selected bond distances and angles are listed in Table 2.

The iron atom is six-coordinate and has a distorted octahedral configuration. The two iodine atoms are *cis* and the two carbonyls are *trans* to each other. The C(1)–Fe(1)–C(2) angle is 165°. The average bond distances of Fe–P (2.215 Å) and Fe–C (1.76 Å) are not significantly different from that observed in the Fe(0) complex with carbonyl and dppm ligands [18]. The carbonyl groups are not colinear with the Fe–C bonds, the angles of Fe–C–O being 175.7° and 170.0°. The nitrogen atom of the diphosphazane ligand possesses a planar configuration.

In contrast with the known $M(CO)_4$(diphosphazane) (M = Mo, W) complexes having coplanar structure of MP_2N ring atoms [19], the four-membered chelate ring Fe(1)/P(1)/N(1)/P(2) in complex **1** is nearly coplanar, with a dihedral angle between P–Fe–P and P–N–P of 3.2°. This slight torsional effect may be caused by the non-bonded interaction between substituent groups. Furthermore, some Fe or Ni complexes containing dppm also show a coplanar four-membered chelate ring [18,20].

Table 3
Fractional coordinates and equivalent isotropic thermal parameters for non-hydrogen atoms of **8**

Atom	*x*	*y*	*z*	B_{eq} (Å^2)
Fe(1)	1.000	0.000	1.000	1.77(4)
Cl(1)	1.0962(4)	−0.2162(4)	1.0235(3)	7.1(1)
P(1)	1.2196(2)	0.0442(2)	1.0242(2)	2.38(5)
P(2)	0.9105(3)	0.0183(2)	1.1659(2)	2.43(5)
C(1)	1.335(1)	0.002(1)	0.9107(8)	3.1(2)
C(2)	0.729(1)	0.084(1)	1.1581(9)	3.5(2)
C(11)	1.255(1)	0.2100(9)	1.0324(8)	2.7(2)
C(12)	1.199(1)	0.299(1)	0.963(1)	4.2(3)
C(13)	1.223(1)	0.426(1)	0.960(1)	5.4(3)
C(14)	1.307(1)	0.458(1)	1.033(1)	7.2(4)
C(15)	1.364(1)	0.368(1)	1.101(1)	5.3(3)
C(16)	1.342(1)	0.243(1)	1.1002(9)	3.9(3)
C(21)	1.3050(9)	−0.0507(9)	1.1258(8)	2.9(2)
C(22)	1.377(1)	−0.173(1)	1.103(1)	3.9(3)
C(23)	1.434(1)	−0.252(1)	1.185(1)	5.6(3)
C(24)	1.422(1)	−0.209(1)	1.277(1)	6.6(3)
C(25)	1.352(1)	−0.092(1)	1.301(1)	5.6(3)
C(26)	1.292(1)	−0.012(1)	1.2230(9)	4.1(3)
C(31)	0.908(1)	−0.1289(9)	1.2450(8)	2.7(2)
C(32)	0.789(1)	−0.162(1)	1.2992(9)	4.0(3)
C(33)	0.789(1)	−0.272(1)	1.356(1)	4.7(3)
C(34)	0.911(1)	−0.352(1)	1.3652(9)	4.6(3)
C(35)	1.028(1)	−0.320(1)	1.3169(9)	3.9(3)
C(36)	1.031(1)	−0.212(1)	1.2565(9)	3.4(2)
C(41)	0.966(1)	0.1282(9)	1.2483(8)	3.2(2)
C(42)	0.999(1)	0.2471(9)	1.2088(9)	3.7(2)
C(43)	1.046(1)	0.326(1)	1.2719(9)	4.2(3)
C(44)	1.057(2)	0.291(1)	1.368(1)	6.0(3)
C(45)	1.029(2)	0.182(1)	1.407(1)	6.5(4)
C(46)	0.980(1)	0.095(1)	1.3475(9)	5.1(3)
Fe(2)	0.4378(3)	0.6346(3)	0.5965(2)	9.32(8)
C	0.3211(9)	0.5650(9)	0.4858(6)	2.1(5)
O	0.6468(7)	0.5300(8)	0.5822(6)	4.5(2)
Cl13	0.4565(7)	0.8313(6)	0.5786(5)	12.1(2)
Cl14	0.3496(5)	0.5900(5)	0.7367(4)	9.3(1)

Anisotropically refined atoms are given in the form of the equivalent isotropic thermal parameter defined as: $(4/3)*[a^2 * B(1, 1) + b^2 * B(2, 2) + c^2 * B(3, 3) + ab(\cos \gamma) * B(1, 2) + ac(\cos \beta) * B(1, 3) + bc(\cos \alpha) * B(2, 3)]$.

Table 4
Selected bond lengths (Å) and angles (deg) for $[FeCl_2(dppe)_2][Fe_2Cl_4(CO)_2]$ (**8**)

Bond lengths			
Fe(1)–P(1)	2.338(2)	Fe(1)–P(2)	2.322(2)
Fe(1)–Cl(1)	2.353(3)		
Fe(2)–C	2.179(6)	Fe(2)–O	2.191(5)
Fe(2)–Cl13	2.112(5)	Fe(2)–Cl14	2.050(4)
C–O	1.38(9)		
Bond angles			
Cl(1)–Fe(1)–Cl(1) [a]	180.0(8)	P(1)–Fe(1)–P(1) [a]	180.0(9)
Cl(1)–Fe(1)–P(1)	85.17(7)	P(1)–Fe(1)–P(2)	96.81(7)
Cl(1)–Fe(1)–P(1) [a]	94.84(7)	P(1)–Fe(1)–P(2) [a]	83.19(7)
Cl(1)–Fe(1)–P(2)	94.64(8)	P(2)–Fe(1)–P(2) [a]	180.0(5)
Cl(1)–Fe(1)–P(2) [a]	85.36(8)		
Fe(1)–P(1)–C(1)	108.9(2)	Fe(1)–P(2)–C(2)	105.1(3)
Fe(1)–P(1)–C(11)	121.9(2)	Fe(1)–P(2)–C(31)	117.5(2)
Fe(1)–P(1)–C(21)	115.4(3)	Fe(1)–P(2)–C(41)	122.1(3)
C–Fe(2)–O	107.6(2)	O–Fe(2)–Cl13	106.6(3)
C–Fe(2)–Cl13	115.3(2)	O–Fe(2)–Cl14	108.4(2)
C–Fe(2)–Cl14	107.7(3)	Cl13–Fe(2)–Cl14	111.0(2)
Fe(2)–C–O	132.9(4)	Fe(2)–O–C	119.5(4)

[a] Symmetrical transformations: $a = (2 - x, -y, 2 - z)$.

2.4. Molecular structure of 8

The crystalline cell of **8** is shown in Fig. 4. Fractional coordinates and equivalent isotropic parameters for non-hydrogen atoms are given in Table 3. Selected bond distances and angles are summarized in Table 4.

An ORTEP diagram of the molecular structure of complex **A** in **8** is shown in Fig. 5. The iron atom lies at the centre of symmetry, octahedrally coordinated by two dppe ligands and two chloride atoms. The dppe ligands have a normal *gauche* conformation. Four phosphorus atoms and the iron atom are coplanar.

The Fe–P distances are 2.338 and 2.322 Å, respectively, slightly longer than those of low-spin complexes, (for example $FeCl_2(depe)_2$ (2.260 Å, depe = $Et_2PCH_2CH_2PEt_2$) [8] and $FeCl_2(dmpe)_2$ (2.241 Å, dmpe = $Me_2PCH_2CH_2PMe_2$) [9]); but they are much shorter than those of high-spin complexes (for example, $FeCl_2(dppen)_2$ (2.675 Å, dppen = $Ph_2PCH{=}CHPPh_2$) [10], $FeCl_2(bdpp)_2$ (2.713 Å, bdpp = $Ph_2PCH_2CH_2PPhCH_2CH_2PPh_2$) [9], $FeCl_2(opdp)_2$ (2.612 Å, opdp = 1,2-$C_6H_4(PPh_2)_2$) [11]). These results suggest that the complex $FeCl_2(dppe)_2$ is low-spin.

The molecular structure of **B** is shown in Fig. 6. Two $FeCl_2$ molecules are bridged by two carbonyls. For each carbonyl, the carbon atom coordinates to an iron atom, and the oxygen atom coordinates to another iron atom. Two $FeCl_2(CO)$ fragments are of central symmetry. The iron atoms show a slightly distorted tetrahedral configuration.

Two iron atoms and two carbonyls are coplanar. Four chloride atoms are also coplanar. The least-squares planes and deviations of the atoms are given in Table 5.

In contrast with some ELHB complexes containing μ-CO bridging carbonyls [14], Fe–C–O (132.9°) and Fe–O–C (119.5°) are not linear.

The Fe–C distance is 2.179 Å, longer than those of complexes containing terminal or bridging carbonyls. The Fe–O distance of 2.191 Å is also longer than the usual Fe–O distances. The long distances of Fe–C and Fe–O indicate a weak interacton between carbonyls and iron atoms. The separation of two iron atoms (3.958 Å) indicates no interaction between them.

3. Experimental section

Unless otherwise stated, all reactions were performed under a nitrogen atmosphere with the use of standard

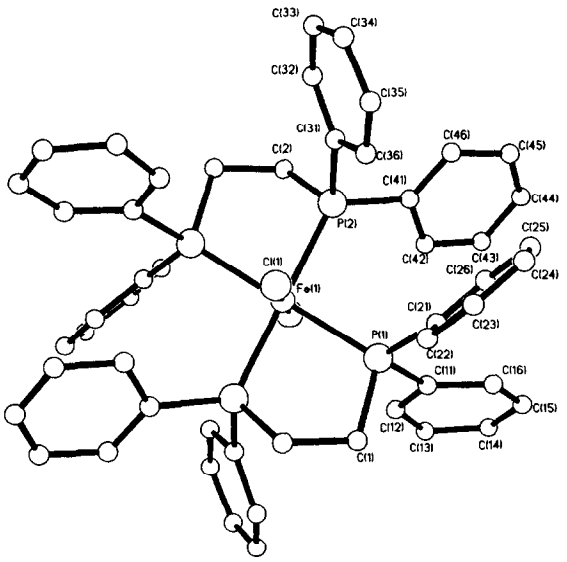

Fig. 5. Molecular structure of $FeCl_2(dppe)_2$ (**8A**).

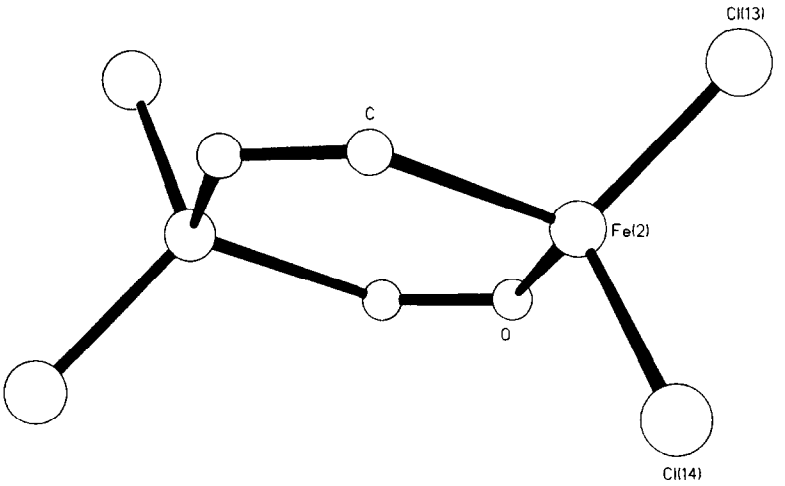

Fig. 6. Molecular structure of $Fe_2Cl_4(CO)_2$ (**8B**).

Schlenk techniques. The solvents were purified by standard methods. $^{i}PrN(PPh_2)_2$, $^{i}BuN(PPh_2)_2$ were prepared by literature methods [19,21].

Infrared spectra were recorded on a WFD-14 spectrometer as KBr discs. The ^{31}P NMR spectra were recorded on a JEOL Fx-90Q spectrometer at 36.19 Hz using H_3PO_4 as external standard and $CDCl_3$ as solvent.

3.1. Preparation of $Fe(CO)_2I_2[^{i}BuN(PPh_2)_2]$ (1)

Reduced iron powder (0.11 g, 2 mmol) and iodine (0.25 g, 1 mmol) were refluxed in tetrahydrofuran (20 ml) for 2 h. The solution was cooled to room temperature and excess iron removed with a magnet. Carbon monoxide was bubbled into the solution, then $^{i}BuN(PPh_2)_2$ (0.44 g, 1 mmol) was added. After the mixture was stirred under carbon monoxide atmosphere for 0.5 h, a dark green precipitate was obtained and filtered to collect the precipitate. The volume of the filtrate was reduced and diethyl ether was added to give further green solid by filtration. The product was recrystallized from CH_2Cl_2/CH_3OH as dark green microcrystals (0.63 g, 80%). M.p. 150°C (dec.). IR: γ (CO), 1990 cm^{-1}. $^{31}P\{^{1}H\}$ NMR: δ (ppm), 115.77. Anal. Found: C, 44.30; H, 3.72; N, 1.32. $C_{30}H_{29}FeI_2NO_2P_2$ Calc.: C, 44.61; H, 3.59; N, 1.73%.

The following complexes were obtained by a similar method.

3.1.1. $Fe(CO)_2I_2[^{i}PrN(PPh_2)_2]$ (4)

Yield 73%. Dark green microcrystals (CH_2Cl_2/CH_3-OH). M.p., 164°C (dec.). IR: γ (CO), 1987 cm^{-1}. $^{31}P\{^{1}H\}$ NMR: δ (ppm), 113.48. Anal. Found: C, 43.57; H, 2.94; N, 1.85. $C_{29}H_{27}FeI_2NO_2P_2$ Calc.: C, 43.88; H, 3.40; N, 1.76%.

3.1.2. $Fe(CO)_2I_2(dppe)$ (6)

Yield 50%. Dark red microcrystals (CH_2Cl_2/CH_3-OH). M.p. 172°C (dec.). IR: γ (CO), 1988 cm^{-1}. $^{31}P\{^{1}H\}$ NMR: δ (ppm), 90.32. Anal. Found: C, 43.91; H, 3.06. $C_{28}H_{24}FeI_2O_2P_2$ Calc.: C, 43.98; H, 3.14%.

3.2. Preparation of $Fe(CO)_2Br_2[^{i}BuN(PPh_2)_2]$ (2)

Reduced iron powder (0.11 g, 2 mmol) was added to a solution of bromine (0.16 g, 1 mmol) in 20 ml of tetrahydrofuran. The mixture was refluxed for 2.5 h, and cooled to room temperature, excess iron was removed with a magnet. Carbon monoxide was bubbled through the solution for 5 min, then $^{i}BuN(PPh_2)_2$ (0.44 g, 1 mmol) was added. The mixture was stirred under carbon monoxide for 2 h to give a dark red solution. The solvent was removed in vacuo and the residue was recrystallized from CH_2Cl_2/CH_3OH to give blue–purple microcrystals (0.43 g, 60%). M.p. 140°C (dec.). IR: γ(CO), 1998 cm^{-1}. $^{31}P\{^{1}H\}$ NMR: δ (ppm), 108.08. Anal. Found: C, 50.44; H, 3.90; N, 2.16. $C_{30}H_{29}Br_2FeNO_2P_2$ Calc.: C, 50.49; H, 4.07; N, 1.96%.

Table 5
Least-squares planes and deviations of the atoms in $Fe_2Cl_4(CO)_2$ (**8B**)

Equation	$0.326(2)X + 0.6504(8)Y - 0.6858(8)Z - 1.15(1) = 0$					
	Fe(2)	−0.011(3)	O	0.016(8)	C	0.016(8)
	O′	−0.0155	C′	0.0165	Fe(2)′	0.0111

The following compounds were prepared by an analogous procedure.

3.2.1. $Fe(CO)_2Br_2[^iPrN(PPh_2)_2]$ (5)

Yield 47%. Grey–green microcrystals (CH_2Cl_2/CH_3OH). M.p. 150°C (dec.). IR: γ (CO), 1995 cm^{-1}. $^{31}P\{^1H\}$ NMR: δ (ppm), 106.75. Anal. Found: C, 49.45; H, 3.62; N, 2.11. $C_{29}H_{27}Br_2FeNO_2P_2$ Calc.: C, 49.78; H, 3.86; N, 2.00%.

3.2.2. $Fe(CO)_2Br_2(dppe)$ (7)

Yield 76%. Red microcrystals (CH_2Cl_2/CH_3OH). M.p. 156–158°C. IR: γ (CO), 1935 cm^{-1}. $^{31}P\{^1H\}$ NMR: δ (ppm), 53.50. Anal. Found: C, 49.73; H, 3.22. $C_{28}H_{24}Br_2FeO_2P_2$ Calc.: C, 50.15; H, 3.58%.

3.3. Preparation of $Fe(CO)_2Cl_2[^iBuN(PPh_2)_2]$ (3)

$FeCl_2 \cdot 4H_2O$ (0.2 g, 1 mmol) was dissolved in tetrahydrofuran (30 ml). Carbon monoxide was bubbled through and $^iBuN(PPh_2)_2$ (0.44 g, 1 mmol) was added. The mixture was stirred under carbon monoxide for 3 h. The solvent was removed in vacuo and the residue recrystallized from $CH_2Cl_2/(C_2H_5)_2O$ to give yellow–green microcrystals (0.28 g, 45%). M.p. 134°C (dec.). IR: γ (CO), 1964 cm^{-1}. $^{31}P\{^1H\}$ NMR: δ (ppm), 93.55. Anal. Found: C, 57.28; H, 4.40; N, 2.59 $C_{30}H_{29}Cl_2FeNO_2P_2$ Calc.: C, 57.69; H, 4.65; N, 2.24%.

3.4. Preparation of $[FeCl_2(dppe)_2][Fe_2Cl_4(CO)_2]$ (8)

$FeCl_2 \cdot 4H_2O$ (0.3 g, 1.5 mmol) was dissolved in tetrahydrofuran (30 ml). Carbon monoxide was bubbled through the solution and dppe (0.4 g, 1 mmol) was added. The mixture was stirred under carbon monoxide for 2 h to give an orange solid, filtered to collect the solid and, after recrystallized from $CH_2Cl_2/(C_2H_5)_2O$, the product was obtained as orange needle crystals (0.52 g, 84%). M.p. 110°C (dec.). IR: γ (CO), 1938 cm^{-1}. $^{31}P\{^1H\}$ NMR: δ (ppm), 55.46. Anal. Found: C, 52.19; H, 4.00. $C_{54}H_{48}Cl_6Fe_3O_2P_2$ Calc.: C, 52.55; H, 3.89%.

3.5. X-ray analysis of 1 and 8

Crystals of each complex suitable for X-ray crystallography were grown from CH_2Cl_2/CH_3OH (**1**) or $CH_2Cl_2/(C_2H_5)_2O$ (**8**). A crystal with suitable size was used to collect the independent reflections on an Enraf-Nonius CAD4 diffractometer with MoK α graphite monochromated radiation ($\lambda = 0.71073$ Å) in the range 2–23°. The measurements were carried out at room temperature (23 ± 1°C) by the ω–2θ scan technique. The reflections with $[I \geqslant 3\sigma(I_1)]$ were considered to be observed and used for the structure analysis. Corrections for Lorentz polarisation and absorption were applied to the data.

The structures of **1** and **8** were solved by direct methods (MULTAN 82). The coordinates of the non-hydrogen atoms were obtained through several difference Fourier syntheses. For the coordinates and anisotropic thermal parameters of the non-hydrogen atoms, full-matrix least-squares refinements were carried out. The highest peaks in the final difference Fourier map were 0.96 and 0.83 e $Å^{-3}$ respectively.

All calculations were performed on a PDP-11/44 computer with SDP-PLUS.

Crystallographic data are summarized in Table 6.

Table 6
Crystallographic data for **1** and **8**

	1	**8**
Formula	$C_{30}H_{29}FeI_2NO_2P_2$	$C_{54}H_{48}Cl_6Fe_3O_2P_4$
FW	807.17	1233.14
Colour	blue–green	yellow
Space group	$P\bar{1}$	$P\bar{1}$
Crystal system	triclinic	triclinic
a (Å)	9.605(2)	9.874(2)
b (Å)	10.295(2)	10.576(1)
c (Å)	17.219(4)	13.347(4)
α (deg)	97.86(2)	86.09(2)
β (deg)	94.98(2)	85.05(2)
γ (deg)	109.16(2)	81.43(1)
Z	2	1
d_{calc} (g cm^{-3})	1.70	1.49
Crystal size (mm^3)	0.1 × 0.2 × 0.25	0.2 × 0.2 × 0.25
μ (cm^{-1})	25.4	12.33
Final R	0.071	0.078
Final Rw	0.080	0.082
No. of unique reflections	4509	3850
No. of observed reflections	1399	2236

4. Supplementary material available

Tables giving fractional coordinates, thermal parameters, and bond distances and angles for **1** and **8** (6 pages) are available, ordering information is given on any current masthead page.

Acknowledgement

We thank the Elemento-Organic Chemistry Laboratory, Nankai University for financial support.

References

[1] A.F. Clifford and A.K. Mukherjee, *Inorg. Chem.*, *2* (1963) 151.
[2] I.A. Coben and F.J. Basolo, *Inorg. Nucl. Chem.*, *28* (1965) 511.
[3] W. Hieber and A. Thalhofer, *Angew. Chem.*, *68* (1956) 679.
[4] M.A. Bennett, G.B. Robertson, I.B. Tomkins and P.O. Whimp, *J. Organomet. Chem.*, *32* (1971) C19.
[5] G. Booth and J. Chatt, *J. Chem. Soc. A*, (1962) 2099.
[6] T.A. Manuel *Inorg. Chem.*, *2* (1963) 854.
[7] G.B. Jacobsen and B.L. Shaw, *J. Chem. Soc., Dalton Trans.*, (1987) 2005.
[8] M. Bacci, S. Midollini, P. Stoppioni and L. Sacconi, *Inorg. Chem.*, *12* (1973) 1801.
[9] M. DiVaira, S. Midollini and L. Sacconi, *Inorg. Chem.*, *20* (1981) 3430.
[10] F. Cecconi, M. DiVaira, S. Midollini, A. Orlandini and L. Sacconi, *Inorg. Chem.*, *20* (1981) 3423.
[11] J.E. Barclay, G.J. Leigh, A. Houlton and J. Silver, *J. Chem. Soc., Dalton Trans.*, (1988) 2865.
[12] M. Aresta, P. Giannoccaro, M. Rossi and A. Sacco *Inorg. Chim. Acta*, *5* (1971) 115.
[13] R.V. Parish and B.F. Riley, *J. Chem. Soc., Dalton Trans.*, (1979) 482.
[14] D.W. Stephan *Coord. Chem. Rev. 95* (1989) 41.
[15] D. Tevault and K. Nakamoto *Inorg. Chem.*, *15* (1976) 1282.
[16] C.W. DeKock, and D.A. VanLeirsburg, *J. Am. Chem. Soc.*, *94* (1972) 3235.
[17] D. Tevault, D.P. Strommen, and K. Nakamoto *J. Am. Chem. Soc.*, *99* (1977) 2997.
[18] F.A. Cotton, K.I. Hardcastle and G.A. Rusholme *J. Coord. Chem.*, (1973) 217.
[19] M.S. Balakrishna, T.K. Prakasha, S.S. Krishnanmurthy, U. Siriwardane and N.S. Hosmane *J. Organomet. Chem.*, *390* (1990) 203.
[20] C. Kruger and Y. Tsay *Acta Crystallogr.*, *1328* (1972) 1941.
[21] Z.Z. Zhang, A. Yu, H.P. Xi, R.J. Wang and H.G. Wang *J. Organomet. Chem.*, *470* (1994) 223.